

A Single Residue in the C1 Domain Sensitizes Novel Protein Kinase C Isoforms to Cellular Diacylglycerol Production*

Received for publication, October 12, 2006, and in revised form, October 26, 2006
Published, JBC Papers in Press, October 27, 2006, DOI 10.1074/jbc.C600268200

Daniel R. Dries^{†S1}, Lisa L. Gallegos^{†S1}, and Alexandra C. Newton^{S2}

From the [†]Biomedical Sciences Graduate Program and ^{S2}Department of Pharmacology, University of California at San Diego, La Jolla, California 92093

The C1 domain mediates the diacylglycerol (DAG)-dependent translocation of conventional and novel protein kinase C (PKC) isoforms. In novel PKC isoforms (nPKCs), this domain binds membranes with sufficiently high affinity to recruit nPKCs to membranes in the absence of any other targeting mechanism. In conventional PKC (cPKC) isoforms, however, the affinity of the C1 domain for DAG is two orders of magnitude lower, necessitating the coordinated binding of the C1 domain and a Ca²⁺-regulated C2 domain for translocation and activation. Here we identify a single residue that tunes the affinity of the C1b domain for DAG- (but not phorbol ester-) containing membranes. This residue is invariant as Tyr in the C1b domain of cPKCs and invariant as Trp in all other PKC C1 domains. Binding studies using model membranes, as well as live cell imaging studies of yellow fluorescent protein-tagged C1 domains, reveal that Trp *versus* Tyr toggles the C1 domain between a species with sufficiently high affinity to respond to agonist-produced DAG to one that is unable to respond to physiological levels of DAG. In addition, we show that while Tyr at this switch position causes cytosolic localization of the C1 domain under unstimulated conditions, Trp targets these domains to the Golgi, likely due to basal levels of DAG at this region. Thus, Trp *versus* Tyr at this key position in the C1 domain controls both the membrane affinity and localization of PKC. The finding that a single residue controls the affinity of the C1 domain for DAG-containing membranes provides a molecular explanation for why 1) DAG alone is sufficient to activate nPKCs but not cPKCs and 2) nPKCs target to the Golgi.

Protein kinase C (PKC)³ is a critical transducer of intracellular signaling pathways, with a variety of outputs, most notably

* This work was supported by National Institutes of Health Grants GM-43154, 2T32 GM-07752, and 2T32 GM-08326. The costs of publication of this article were defrayed in part by the payment of page charges. This article must therefore be hereby marked "advertisement" in accordance with 18 U.S.C. Section 1734 solely to indicate this fact.

¹ These authors contributed equally to this work.

² To whom correspondence should be addressed: Dept. of Pharmacology, University of California at San Diego, 9500 Gilman Dr., 0721, La Jolla, CA 92093-0721. Tel.: 858-534-4527; Fax: 858-822-5888; E-mail: anewton@ucsd.edu.

³ The abbreviations used are: PKC, protein kinase C; CFP, cyan fluorescent protein; cPKC, conventional PKC; DAG, diacylglycerol; GST, glutathione S-transferase; FRET, fluorescence resonance energy transfer; nPKC, novel PKC; PDBu, phorbol-12,13-dibutyrate; PMA, phorbol-12-myristate-13-acetate; PM-CFP, plasma membrane-targeted CFP; PG, phosphatidylglycerol; PS, phosphatidylserine; YFP, yellow fluorescent protein.

tumor promotion (1, 2). The hallmark of PKC activation is its translocation to membranes (3). This translocation is mediated through the ligand-dependent engagement of two membrane-targeting modules: the C1 (ligand: diacylglycerol or DAG) and C2 (ligand: Ca²⁺) domains. The regulatory domains vary within the PKC family, which is subdivided into three groups based on regulation. The conventional PKC isoforms (cPKCs: α , β /II, γ) contain two tandem C1 domains and one conventional C2 domain; consequently, cPKCs are regulated both by DAG and Ca²⁺. The novel isoforms (nPKCs: δ , ϵ , η , and θ) contain two tandem C1 domains and a non-Ca²⁺/membrane-binding novel C2 domain; consequently, nPKCs are regulated only by DAG. Atypical PKCs (aPKCs: ι and ζ) contain a single non-DAG-binding ("atypical") C1 domain and no C2 domain; as a result, aPKCs are regulated by neither DAG nor Ca²⁺ (4).

The C1 domain is an ~8-kDa domain that binds DAG or the potent DAG-mimicking phorbol esters, such as phorbol-12-myristate-13-acetate (PMA) and phorbol dibutyrate (PDBu) (5). Structural studies have established that all C1 domains have a similar fold (6–11). An "unzipped" β sheet forms a groove lined by hydrophobic residues in which membrane-embedded diacylglycerol or phorbol esters bind (7). Membrane interaction is also facilitated by a ring of positive charges around the middle of the domain that potentially interacts with phosphatidylserine (PS) and other anionic lipids (12).

Nearly all C1 domains have been shown to bind PS (13), but their affinity for ligand (DAG/phorbol esters) varies substantially (14). The C1 domain of nPKCs has an intrinsic affinity for DAG-containing membranes 2 orders of magnitude higher than that of the C1 domain of cPKCs, allowing nPKCs to respond to agonists that trigger diacylglycerol production alone (15). In contrast, cPKCs must be pretargeted to membranes by their C2 domain in response to an elevation of intracellular Ca²⁺ to respond to DAG (16). The molecular basis by which nPKC C1 domains bind to DAG membranes with two orders of magnitude higher affinity than those of cPKC C1 domains has not been elucidated.

In this report, we identify a single conserved residue at position 22 in the C1 domain that tunes its affinity for DAG-containing membranes. Our findings provide a molecular basis for why nPKCs respond to DAG alone, whereas cPKCs require the coordinated elevation of Ca²⁺.

EXPERIMENTAL PROCEDURES

Materials—1-Palmitoyl-2-oleoyl-*sn*-glycero-3-phosphocholine, 1-palmitoyl-2-oleoyl-*sn*-glycero-3-phosphoserine, 1-palmitoyl-2-oleoyl-*sn*-glycero-3-phosphoglycerol, and 1,2-*sn*-dioleoylglycerol in chloroform were from Avanti Polar Lipids, Inc. Tritiated 1,2-dipalmitoyl-*sn*-glycero-3-phosphocholine was from American Radiochemical Co. [γ -³²P]ATP was from PerkinElmer Life Sciences. PMA, PDBu, and BAPTA/AM were from CalBiochem. Glutathione-Sepharose 4B and PreScission Protease were from Amersham Biosciences. Electrophoresis reagents were from Bio-Rad. Oligonucleotides were from GenBase, Inc. Restriction

enzymes were from New England Biolabs, Inc. All other reagents and chemicals were reagent-grade.

Sequence Alignments—Sequences of the C1 domains of PKC isoforms (13) were aligned using CLUSTALW from the LaserGene 6 software package (DNASTAR, Inc.). Residues that contact ligand in the structure of C1b δ with phorbol were taken from the LIGPLOT file provided through the Protein Data Bank (PDB) repository (PDB ID: 1PTR).

Construction of Plasmids and Protein Purification—For bacterial expression, C1b β was cloned into pGEX-KG as described (17). C1b δ (Gln-221 to Ala-290) and C1b β were subcloned into pGEX-6P3, in which the Tyr-22 \rightarrow Trp mutation was introduced. For mammalian expression, all constructs were cloned into pcDNA3. PM-CFP was cloned as described (18). YFP was fused to the 3' end of C1b β (Pro-93 to Gly-152) and C1b δ (Phe-225 to Gly-281) to make C1b β -YFP and C1b δ -YFP. These constructs were used to produce the mutants Tyr22Trp (C1b β) and Trp-22 \rightarrow Tyr (C1b δ). YFP was fused to the 3' end of PKC β II or δ , and Tyr123Trp or Trp252Tyr mutations were introduced, respectively. Rat PKC β II and murine PKC δ isoforms were used in these studies. All mutations were made using QuikChange (Stratagene). Wild-type C1b β was expressed in bacteria and purified as described previously (17). The C1b β II-Y123W and C1b δ domains were purified similarly (17), with the substitution of PreScission Protease for thrombin.

Sucrose-loaded Vesicle Binding Assay—Lipid vesicles were prepared and PMA was incorporated into these vesicles as described (15). The final concentration of lipid was determined by phosphate analysis as described (19). The binding of the C1b domain to sucrose-loaded large unilamellar vesicles was measured as described (20). To normalize data between 0 and 100% bound, curves were fitted to Equation 1,

$$\text{Fraction bound} = (n*[L]^H)/([L]^H + K_d^H) + \text{int} \quad (\text{Eq. 1})$$

where K_d is the apparent equilibrium constant, $[L]$ is the lipid concentration, H is the Hill coefficient, n is the range of apparent percent bound, and int is the y intercept. Experiments were performed in triplicate. Measurements at each lipid concentration were averaged, and data were fitted to one master S.E.-weighted plot of the following form,

$$\text{Fraction bound} = [L]^H/([L]^H + K_d^H) \quad (\text{Eq. 2})$$

where the terms represent the same parameters as in Equation 1. All curve fitting was done using Kaleidagraph v5.32.

Cell Culture—COS7 cells were plated in Dulbecco's modified Eagle's medium (Cellgro) containing 10% fetal bovine serum and 1% penicillin/streptomycin at 37 °C in 5% CO₂. Cells were plated in 35-mm imaging dishes at 60% confluence and transfected using FuGENE 6 (Roche Diagnostics). Cells were cotransfected with PM-CFP and C1b-YFP constructs for translocation studies. For localization experiments, the YFP-tagged constructs were transfected alone. Cells were allowed to grow for 12–24 h post-transfection before imaging. For kinase activity assays, cells were transfected with full-length YFP-tagged constructs (to monitor expression) and allowed to grow for 48 h post-transfection before harvesting.

Cell Imaging—Cells were imaged as described previously (18, 21). Because of cell-to-cell variability in CFP and YFP expres-

sion, the dynamic range varied from cell to cell. However, treatment with phorbol esters caused maximal membrane binding of each domain (Fig. 1C). Therefore, the responses to DAG generation via UTP were calibrated to the dynamic range of the cell by dividing each point by the maximal response elicited by PDBu. Thus, the data are presented in relative translocation units.

Kinase Assay—Lysates from untransfected COS7 cells or COS7 cells transfected with PKC β II, PKC β II-Y123W, or PKC δ were assayed for PKC activity by monitoring phosphorylation of a synthetic peptide as described (22). Non-activating conditions contained 20 mM HEPES (pH 7.5) and 2 mM EGTA. Activating conditions contained 140 μ M PS, 3.8 μ M DAG, and either 2 mM CaCl₂ (total PKC activity) or 2 mM EGTA (Ca²⁺-independent PKC activity).

Molecular Modeling—The structure of the C1 domain was visualized and manipulated using Swiss-PdbViewer, v3.7. Coordinates for C1-Raf (1FAR), C1b-PKC γ (1TBN), and C1b-PKC δ (1PTQ) were taken from the PDB repository (PDB ID numbers in parentheses). The C1 domain of human PKC ζ was modeled on the C1 domains of DGK δ (1R79), Ksr (1KBE), β 2-chimaerin (1XA6), munc-13 (1Y8F), PKC δ , PKC γ , and Raf, using Swiss-PdbViewer (23–25).

RESULTS AND DISCUSSION

The C1 domains of nPKCs bind DAG-containing membranes with 2 orders of magnitude higher affinity than those of cPKCs (15). Alignment of the sequences of C1 domains of cPKCs and nPKCs revealed that the residue at position 22 is invariant as Trp in all C1 domains except the C1b domains of cPKCs, where it is invariant as Tyr (Fig. 1A). This residue lies along one of the two loops that bind ligand and is on a surface that interacts with the membrane (12). Thus this is a candidate to modulate ligand-dependent membrane affinity.

To test the hypothesis that position 22 controls the affinity of the C1b domain for lipid membranes, we first mutated Tyr-22 to Trp in the C1b domain of the cPKC β I/II (C1b β -Y22W) and measured the binding of the bacterially purified wild-type and mutant domains to lipid vesicles containing 30 mol % PS and 5 mol % DAG (Fig. 1B, *filled symbols*). Wild-type C1b β (C1b β -WT) bound to vesicles containing 5 mol % DAG with a K_d of $780 \pm 50 \mu$ M (*filled diamonds*). On the other hand, the mutant C1b β -Y22W bound with 31-fold higher affinity to vesicles of the same composition ($K_d = 24 \pm 1 \mu$ M, *filled squares*). Binding was dependent on the presence of DAG, as the domain did not bind to 500 μ M lipid vesicles containing 30 mol % PS and 0 mol % DAG (data not shown). We next measured the binding of these two domains to vesicles containing 30 mol % PS and 1 mol % PMA (Fig. 1B, *open symbols*). C1b β -WT and -Y22W bound with the same affinity to vesicles containing 1 mol % PMA (K_d values of 35 ± 3 and $35 \pm 2 \mu$ M, *open diamonds* and *squares*, respectively). These data reveal that mutation of Tyr-22 to Trp in the C1 domain of PKC β converts the domain from a low affinity to a high affinity DAG-binding module.

We next tested whether the isolated C1b domain of the nPKC δ (C1b δ), which has a Trp at position 22, also has higher intrinsic affinity for DAG-containing membranes than C1b β . We used a GST-tagged construct for C1b δ , as removal of the

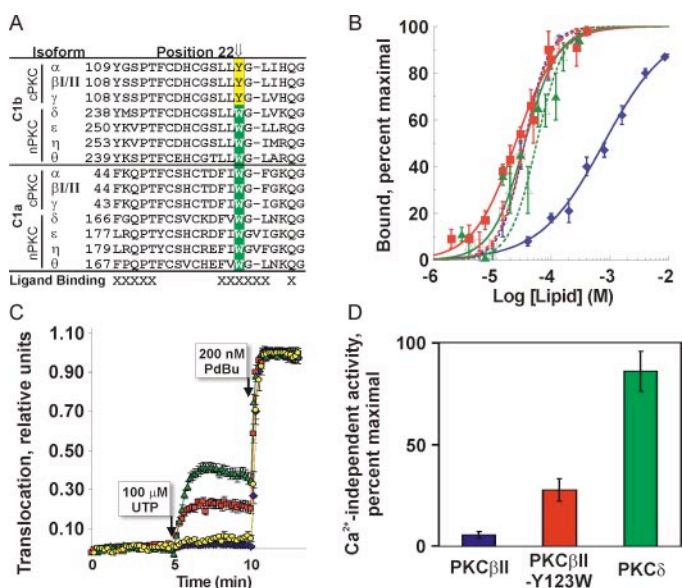


FIGURE 1. Residue 22 tunes binding of the C1b domain to DAG membranes *in vitro* and *in vivo* and affects kinase activity. *A*, sequence alignment of the C1 domains of cPKC and nPKC isoforms. Position 22 is boxed in yellow for Tyr and green for Trp. Residues that contact phorbol and/or form the hydrophobic wall of the groove in which DAG or phorbol binds are marked below with an "X." *B*, binding of C1b β -WT (blue diamonds) and -Y22W (red squares) and GST-C1b δ (green triangles) to lipid vesicles containing 30 mol % PS and either 5 mol % DAG (filled symbols) or 1 mol % PMA (open symbols). Each data point represents the mean of triplicate experiments \pm S.E. *C*, *in vivo* translocation of C1b domains to membranes. COS7 cells were cotransfected with PM-CFP and the indicated YFP-tagged C1b domain constructs: C1b β (blue diamonds), C1b β -Y22W (red squares), C1b δ (green triangles), and C1b δ -W22Y (yellow circles). The relative translocation in response to UTP (100 μ M) and PDBu (200 nM) treatment was calculated and plotted as a function of time. Data represent the average \pm S.E. of 10–15 cells from three independent experiments. *D*, lysates from COS7 cells transfected with PKC β II, PKC β II-Y123W, or PKC δ were assayed for PKC activity in the presence of PS, DAG, and either Ca²⁺ (total PKC activity) or EGTA (calcium-independent PKC activity). Ca²⁺-independent PKC activity was calculated as a percent of total activity; total activity was comparable for both PKC β II constructs and typically slightly lower for the PKC δ construct. These data represent the relative activity of the overexpressed kinases in response to lipid cofactors in the absence of Ca²⁺. Data represent the average \pm S.D. from three experiments.

GST tag greatly reduced the stability of the protein. GST-C1b δ bound to vesicles containing 5 mol% DAG and 1 mol % PMA with K_d values of 35 ± 3 and 56 ± 6 μ M, respectively (Fig. 1B, triangles). Low, but pure, amounts of untagged C1b δ showed that the GST tag had no effect on the affinity of the C1b δ for DAG- or PMA-containing membranes (data not shown). Moreover, while C1b β -WT showed a 110-fold preference for PMA over DAG on an equimolar basis (Fig. 1B, open versus closed diamonds), C1b β -Y22W and GST-C1b δ showed modest 3.6- and 3.1-fold selectivities for PMA over DAG, respectively (Fig. 1B, open versus closed squares for C1b β -Y22W and triangles for GST-C1b δ).

We previously observed that the C1 domain exhibits selectivity among anionic lipids in the presence of DAG, with preference for PS over phosphatidylglycerol (PG) (17). Since residue 22 is important for sensitizing the C1b domain to DAG, this position should also allow the domain to discriminate between PS and PG. Therefore, we measured the affinity of the C1b β -WT, C1b β -Y22W and GST-C1b δ domains for membranes containing 30 mol % PS or PG and 5 mol % DG or PMA. Wild-type C1b β showed 2-fold selectivity for PS over PG, regardless

TABLE 1
Binding constants (K_d) for the interaction of the C1b domain with membranes

Apparent K_d values were calculated from binding curves as described under "Experimental Procedures." Data shown here are for lipid vesicles consisting of 5 mol % DAG or PMA and 30 mol % PS or PG. K_d (in μ M) is presented as the average of three experiments \pm S.E.

Ligand	K_d (μ M)					
	C1b β		C1b β -Y22W		C1b δ	
	DAG	PMA	DAG	PMA	DAG	PMA
PS	780 ± 50	11.5 ± 0.5	24 ± 1	5.3 ± 0.5	35 ± 3	8.5 ± 0.6
PG	1690 ± 60	22 ± 1	130 ± 10	6.0 ± 0.9	700 ± 200	25 ± 3
PG:PS	2.2 ± 0.2	1.9 ± 0.1	5.4 ± 0.5	1.1 ± 0.2	20 ± 6	2.9 ± 0.4

of whether the ligand was DAG or PMA (Table 1). Trp-containing C1 domains, however, showed high selectivity for PS, although only in the context of DAG membranes (5- and 20-fold selectivity for C1b β -Y22W and GST-C1b δ , respectively). On the other hand, these proteins had no or 3-fold selectivity for PS for C1b β -Y22W and GST-C1b δ , respectively, in the context of PMA-containing membranes. Taken together, then, these data reveal that Trp at position 22 increases the affinity of C1b β for DAG-containing membranes, reduces selectivity between PMA and DAG, and increases DAG-dependent PS selectivity.

To monitor the real-time membrane translocation of isolated C1b domains in live cells, we fused YFP to the C terminus of C1b β and C1b δ . We also generated YFP fusion constructs for these two C1b domains containing point mutations reversing the identity of residue 22: C1b β -Y22W and C1b δ -W22Y. We cotransfected COS7 cells with CFP that had been targeted to the plasma membrane (PM-CFP) and the indicated YFP-tagged C1b construct; translocation to the plasma membrane was monitored as an increase in the ratio of FRET-based YFP emission: CFP emission (FRET ratio) (21).

UTP, acting through endogenous P2Y receptors, stimulates the production of DAG at the plasma membrane via phospholipase C-mediated lipid hydrolysis (26). Fig. 1C shows that stimulation of COS7 cells with UTP (100 μ M) resulted in an increase in FRET ratio, which was further increased to maximal translocation following addition of PDBu (200 nM). Upon stimulation of COS7 cells with UTP, C1b β did not significantly translocate to membranes (Fig. 1C, blue diamonds). In contrast, UTP stimulation caused robust translocation of C1b δ (Fig. 1C, green triangles). Consistent with *in vitro* binding data (Fig. 1B), C1b β -Y22W responded to UTP (Fig. 1C, red squares), resulting in a 10-fold increase in DAG binding at the plasma membrane relative to C1b β -WT (Fig. 1C, blue diamonds). Conversely, mutating Trp-22 to Tyr in C1b δ (C1b δ -W22Y) reduced the translocation in response to UTP 10-fold relative to C1b δ without altering the maximal translocation driven by PDBu (Fig. 1C, yellow circles). These data reveal that Trp versus Tyr at position 22 in the C1b domain renders the domain responsive to DAG generated by receptor-mediated phospholipid hydrolysis.

To determine whether binding differences arising from changes in the C1b domain affected the cofactor dependence of the full-length kinase, we generated a full-length PKC β II construct in which Tyr-123 (position 22 of the C1b domain) was mutated to Trp (PKC β II-Y123W). We transfected COS7 cells with either this mutant construct, wild-type PKC β II, or PKC δ

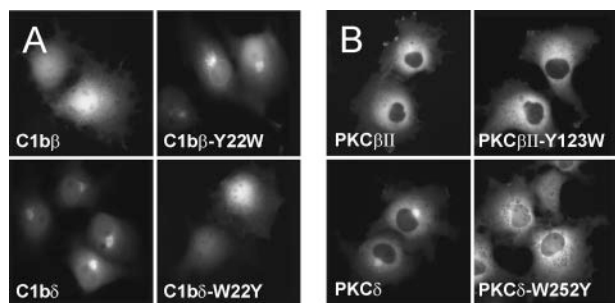


FIGURE 2. Residue 22 affects localization of the C1b domain (A) and full-length PKC (B). A, representative images of COS7 cells transfected with YFP-tagged C1b domains: C1b β (top left), C1b β -Y22W (top right), C1b δ (lower left), and C1b δ -W22Y (lower right). B, representative images of COS7 cells transfected with YFP-tagged full-length PKC: PKC β II (top left), PKC β II-Y123W (top right), PKC δ (lower left), and PKC δ -W252Y (lower right). Mutated residues correspond to position 22 of the C1b domain in the full-length protein. Data are representative of at least three independent experiments.

and assayed kinase activity from the detergent-soluble lysates compared with untransfected control cells. We assayed PKC activity in the presence of PS, DAG, and either Ca²⁺ (for total PKC activity) or EGTA (for Ca²⁺-independent activity), and Ca²⁺-independent activity was calculated as a percent of total PKC activity. Fig. 1D shows the Ca²⁺-independent activity of PKC β II, PKC β II-Y123W, and PKC δ . Consistent with the standard model where Ca²⁺, DAG, and PS are required for full activation of cPKCs (27), PKC β II had minimal (6%) activity in the absence of Ca²⁺. In contrast, PKC δ was activated to near maximal levels in the absence of Ca²⁺, consistent with the Ca²⁺ independence of novel PKC isoforms (27). Strikingly, the single point mutation of Y123W in PKC β II was sufficient to confer significant Ca²⁺-independent activity (28% of maximal activity). These results are consistent with the tighter membrane affinity conferred by Trp *versus* Tyr in the C1b domain, which results in reduced dependence on the C2 domain (and hence Ca²⁺) for activation and is consistent with our previous studies, which showed that activation of PKC depends upon the affinity by which PKC binds to membranes (17). This provides a molecular explanation for why novel PKC isoforms are able to respond to DAG alone, while conventional PKC isoforms require pretargeting by Ca²⁺ via their C2 domains for translocation and activation (15, 16).

Translocation of different PKC isoforms to discrete subcellular regions is an important mechanism for achieving specificity in PKC signaling. While the typical site of signaling for cPKCs is the plasma membrane (28), localization at endomembranes, particularly the Golgi, has been shown to be critical for PKC δ activity (29). We observed striking differences in the localization of the isolated, YFP-tagged C1b β and C1b δ : C1b β was localized diffusely throughout the cell (Fig. 2A, upper left panel), while C1b δ was concentrated at a juxtannuclear region resembling Golgi membranes (Fig. 2A, lower left panel). Localization at the Golgi was confirmed by treatment with brefeldin A, which abolished the juxtannuclear concentration of C1b δ (data not shown). Moreover, the reversion mutants C1b β -Y22W and C1b δ -W22Y showed a complete reversal of the subcellular localization of their wild-type counterparts (Fig. 2A, right panels). A previous study reported constitutive Golgi localization of the C1b domain of the nPKC θ in unstimulated cells; this localization was redistributed to the cytosol upon

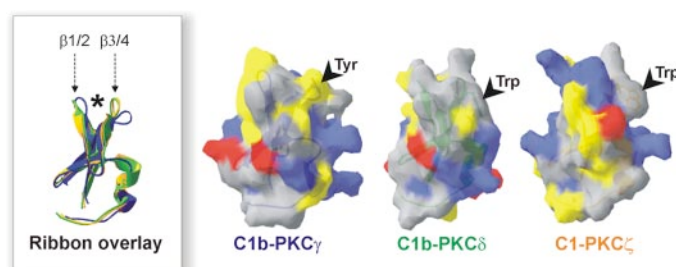


FIGURE 3. The ability of the C1 domain to bind DAG arises from modulation of the width and surface properties of the loops surrounding the hydrophobic DAG-binding cleft. Shown are a ribbon diagram overlay and molecular surfaces of C1b-PKC γ (blue), C1b-PKC δ (green), and C1-PKC ζ (orange). Phorbol binds between the two loops at the top of the domain as indicated with an asterisk. The identity of residue 22 is marked with an arrowhead. Surface coloring scheme is as follows: blue, basic; red, acidic; yellow, polar; gray, nonpolar.

inhibition of phospholipase C or phosphatidic acid phosphatase (30). Thus, the targeting effects of position 22 are likely due to DAG-dependent membrane binding.

Next, we tested whether having a Tyr or Trp at position 22 also affected the localization of either full-length PKC β II or PKC δ . PKC δ prelocalized to juxtannuclear membranes, while PKC β II was basally cytosolic (Fig. 2B, left panels). Consistent with data from the isolated C1b domains, basal Golgi localization of the full-length PKC δ was greatly diminished upon mutation of Trp-252 (position 22 of the C1b domain) to Tyr (Fig. 2B, lower right panel). However, mutation of Tyr-123 to Trp in PKC β II did not cause any change in its localization, as PKC β II remained cytosolic (Fig. 2B, upper panels). Thus, merely increasing the affinity of the C1b domain for DAG is not sufficient to determine the subcellular distribution of PKC. This suggests that other determinants control cPKC localization. For example, the Ca²⁺-binding C2 domain of cPKCs, a feature absent from nPKCs, may override targeting to the Golgi (31, 32). Thus, in addition to affecting PKC function by regulating activation in response to DAG, position 22 of the C1b domain may also regulate DAG-dependent prelocalization of novel PKC isoforms. Taken together, these data suggest a model of activation in which low DAG levels allow pretargeting of PKC δ to the Golgi through the C1b domain, while an additional agonist-stimulated increase in DAG shifts the equilibrium to full binding and full activation.

To gain insight into how Trp *versus* Tyr at position 22 controls the affinity of the C1 domain for DAG-containing membranes, we compared the backbone structures and molecular surfaces of several C1 domains (Fig. 3). We chose representatives of three C1 groups for modeling studies: those that bind DAG membranes with relatively high affinity (C1b δ), those that bind DAG membranes with relatively low affinity (C1b γ , a surrogate for C1b β , with which C1b γ shares 80% identity and 92% similarity), and those that do not bind DAG (C1 ζ). As shown in Fig. 3, comparison of the C1b domains of PKC γ , - δ , and - ζ reveals large movements within the β 3/4 loop (left panel). The β 1/2 and β 3/4 loops form the phorbol/DAG-binding pocket and contain the ligand- and membrane-binding determinants (7, 13). Residue 22 lies at the apex of this highly mobile β 3/4 loop, in keeping with its role as a critical regulator for the ability of the C1 domain to bind DAG.

Numerous elegant studies delineating the residues in the C1 domain involved in ligand binding have identified residue 22 as participating in DAG-dependent membrane binding (8, 14, 33, 34), yet the mechanism by which this position controls binding to membranes has not been clear. Our modeling studies suggest that position 22 may regulate the size of the ligand-binding pocket (Fig. 3). The phenol ring of Tyr-22 in C1b γ lies in a very different orientation relative to the membrane compared with the indole ring of Trp-22 in C1b δ . Moreover, these two amino acids are known to be positioned very differently at the water/lipid bilayer interface (35, 36), suggesting that mobility in the β 3/4 loop may dictate the width and depth of the ligand-binding pocket. Indeed, several studies have shown flexibility within this loop, whereas the rest of the structure tends to remain static (7, 8, 37). The presence of two highly conserved Gly residues within the β 3/4 loop (Gly-23 and Gly-28) suggests that such flexibility is not only possible but may also be required for function. Particularly relevant to our study, the ligand-binding cavity in C1b δ is narrow and deep, while that of the non-DAG responsive C1b γ is wide and shallow. Thus, whereas the smaller DAG can bind well to C1b δ , only the larger phorbol esters can make hydrophobic contacts across the wide gorge of C1b γ .

Curiously, the C1 domain of PKC ζ has Trp at position 22, yet it still does not bind DAG. Rather, C1 ζ appears to lose the ability to bind DAG by sterically and electrostatically occluding the ligand-binding pocket through substitution of hydrophobic residues (gray) for large basic amino acids (blue) (Fig. 3). Indeed, Blumberg and co-workers have shown that mutation of Asn-7, Ser-10, Pro-11, and Leu-20 in the β 1/2 and β 3/4 loops to arginine in C1b δ results in almost complete loss of binding to phorbol ester-containing membranes, while the reverse mutations in C1 ζ confer phorbol ester responsiveness (38).

CONCLUSION

In this study, we identify Trp *versus* Tyr at residue 22 of the C1b domain as a molecular switch that controls whether PKC isoforms can respond to DAG alone or whether the coordinated binding of a second membrane-targeting module (*i.e.* the C2 domain of cPKCs) is required to confer responsiveness to agonist. Our findings provide a molecular basis for why nPKCs respond to DAG alone, whereas cPKCs require the coordinated elevation of Ca²⁺. This cautions against drawing physiological conclusions when substituting phorbol esters for DAG in the context of cellular signaling, an idea that has also been suggested by other groups (33). Taken further, our results also suggest that therapeutic compounds designed to target the C1 domain of a specific isoform should more closely resemble DAG than phorbol, an approach taken by Blumberg and co-workers (39).

REFERENCES

1. Koivunen, J., Aaltonen, V., and Peltonen, J. (2005) *Cancer Lett.*
2. Mellor, H., and Parker, P. J. (1998) *Biochem. J.* **332**, 281–292

3. Nishizuka, Y. (1995) *FASEB J.* **9**, 484–496
4. Newton, A. C. (2001) *Chem. Rev.* **101**, 2353–2364
5. Colon-Gonzalez, F., and Kazanietz, M. G. (2006) *Biochim. Biophys. Acta.* **1761**, 827–837
6. Zhou, M., Horita, D. A., Waugh, D. S., Byrd, R. A., and Morrison, D. K. (2002) *J. Mol. Biol.* **315**, 435–446
7. Zhang, G., Kazanietz, M. G., Blumberg, P. M., and Hurley, J. H. (1995) *Cell* **81**, 917–924
8. Xu, R. X., Pawelczyk, T., Xia, T. H., and Brown, S. C. (1997) *Biochemistry* **36**, 10709–10717
9. Mott, H. R., Carpenter, J. W., Zhong, S., Ghosh, S., Bell, R. M., and Campbell, S. L. (1996) *Proc. Natl. Acad. Sci. U. S. A.* **93**, 8312–8317
10. Canagarajah, B., Leskow, F. C., Ho, J. Y., Mischak, H., Saidi, L. F., Kazanietz, M. G., and Hurley, J. H. (2004) *Cell* **119**, 407–418
11. Shen, N., Guryev, O., and Rizo, J. (2005) *Biochemistry* **44**, 1089–1096
12. Hurley, J. H., and Meyer, T. (2001) *Curr. Opin. Cell Biol.* **13**, 146–152
13. Hurley, J. H., Newton, A. C., Parker, P. J., Blumberg, P. M., and Nishizuka, Y. (1997) *Protein Sci.* **6**, 477–480
14. Stahelin, R. V., Digman, M. A., Medkova, M., Ananthanarayanan, B., Rafter, J. D., Melowic, H. R., and Cho, W. (2004) *J. Biol. Chem.* **279**, 29501–29512
15. Giorgione, J. R., Lin, J. H., McCammon, J. A., and Newton, A. C. (2006) *J. Biol. Chem.* **281**, 1660–1669
16. Nalefski, E. A., and Newton, A. C. (2001) *Biochemistry* **40**, 13216–13229
17. Johnson, J. E., Giorgione, J., and Newton, A. C. (2000) *Biochemistry* **39**, 11360–11369
18. Violin, J. D., Zhang, J., Tsien, R. Y., and Newton, A. C. (2003) *J. Cell Biol.* **161**, 899–909
19. Bartlett, G. R. (1959) *J. Biol. Chem.* **234**, 466–468
20. Mosior, M., and Newton, A. C. (1995) *J. Biol. Chem.* **270**, 25526–25533
21. Gallegos, L. L., Kunkel, M. T., and Newton, A. C. (2006) *J. Biol. Chem.* **281**, 30947–30956
22. Edwards, A. S., Faux, M. C., Scott, J. D., and Newton, A. C. (1999) *J. Biol. Chem.* **274**, 6461–6468
23. Peitsch, M. (1995) *Bio/Technology* **13**, 658–660
24. Schwede, T., Kopp, J., Guex, N., and Peitsch, M. C. (2003) *Nucleic Acids Res.* **31**, 3381–3385
25. Guex, N., and Peitsch, M. C. (1997) *Electrophoresis* **18**, 2714–2723
26. Insel, P. A., Ostrom, R. S., Zambon, A. C., Hughes, R. J., Balboa, M. A., Shehna, D., Gregorian, C., Torres, B., Firestein, B. L., Xing, M., and Post, S. R. (2001) *Clin. Exp. Pharmacol. Physiol.* **28**, 351–354
27. Newton, A. C. (2003) *Biochem. J.* **370**, 361–371
28. Saito, N. (2003) *Methods Mol. Biol.* **233**, 93–103
29. Brodie, C., and Blumberg, P. M. (2003) *Apoptosis* **8**, 19–27
30. Carrasco, S., and Merida, I. (2004) *Mol. Biol. Cell* **15**, 2932–2942
31. Rodriguez-Alfaro, J. A., Gomez-Fernandez, J. C., and Corbalan-Garcia, S. (2004) *J. Mol. Biol.* **335**, 1117–1129
32. Feng, X., Becker, K. P., Stribling, S. D., Peters, K. G., and Hannun, Y. A. (2000) *J. Biol. Chem.* **275**, 17024–17034
33. Ananthanarayanan, B., Stahelin, R. V., Digman, M. A., and Cho, W. (2003) *J. Biol. Chem.* **278**, 46886–46894
34. Wang, Q. J., Fang, T. W., Nacro, K., Marquez, V. E., Wang, S., and Blumberg, P. M. (2001) *J. Biol. Chem.* **276**, 19580–19587
35. Killian, J. A., and von Heijne, G. (2000) *Trends Biochem. Sci.* **25**, 429–434
36. Khandwala, A. S., and Kasper, C. B. (1971) *Biochim. Biophys. Acta* **233**, 348–357
37. Pak, Y., Enyedy, I. J., Varady, J., Kung, J. W., Lorenzo, P. S., Blumberg, P. M., and Wang, S. (2001) *J. Med. Chem.* **44**, 1690–1701
38. Pu, Y., Peach, M. L., Garfield, S. H., Wincovitch, S., Marquez, V. E., and Blumberg, P. M. (2006) *J. Biol. Chem.* **281**, 33773–33788
39. Marquez, V. E., and Blumberg, P. M. (2003) *Acc. Chem. Res.* **36**, 434–443